Experimental Implementation of Spatial $\mathcal{H}_\infty$ Control on a Piezoelectric-Laminate Beam

Dunant Halim, *Student Member, IEEE,* and S. O. Reza Moheimani, *Senior Member, IEEE*

***Abstract*—This paper is aimed to develop a feedback controller that suppresses vibration of flexible structures. The controller is designed to minimize the spatial $\mathcal{H}_\infty$ norm of the closed-loop system. This technique guarantees average reduction of vibration throughout the entire structure. A feedthrough term is incorporated into the truncated flexible-structure model to compensate for the neglected dynamics in the finite-dimensional model. Adding the feedthrough term reduces the uncertainty associated with the truncated model, which is instrumental in ensuring the robustness of the closed-loop system. The controller is applied to a simply-supported piezoelectric-laminate beam and is validated experimentally to show the effectiveness of the proposed controller in suppressing structural vibration. It is shown that the spatial $\mathcal{H}_\infty$ control has an advantage over the pointwise $\mathcal{H}_\infty$ control in minimizing the vibration of the entire structure. This spatial $\mathcal{H}_\infty$ control methodology can also be applied to more general structural vibration suppression problems.**

***Index Terms*—Flexible structures, piezoelectric actuators, piezoelectric sensors, smart structures, spatial control, vibration control.**

I. Introduction

VIBRATION is a natural phenomena that may occur in all dynamic systems. Vibration can be detrimental to structural performance and stability, and so, it is important to find a means of suppressing structural vibrations. In this paper, we describe a controller design framework for suppressing the unwanted structural vibrations in flexible structures.

Flexible structures are distributed parameter systems. Therefore, vibration of each point is dynamically related to the vibration of every other point over the structure. If a controller is designed with a view to minimizing structural vibrations at a limited number of points, it could have negative effects on vibration profile of the rest of the structure. The concept of spatial $\mathcal{H}_\infty$ control was first introduced by the second author in [1] for the purpose of suppressing structural vibration over the entire structure. This paper presents experimental implementation of this concept on a piezoelectric-laminate beam for the first time.

Based on this concept, the controller is designed such that the spatial $\mathcal{H}_\infty$ norm of the closed-loop system is minimized. Minimizing the spatial $\mathcal{H}_\infty$ norm of the system will guarantee vibration suppression over the entire structure in an average sense. This spatial $\mathcal{H}_\infty$ control problem can be solved by finding an equivalent system representation that allows a standard $\mathcal{H}_\infty$ control optimization problem to be solved instead.

Distributed systems have theoretically an infinite number of modes and are represented by infinite-dimensional models. In [2]–[4], infinite-dimensional controllers are obtained from the infinite-dimensional models. Finite-dimensional controllers are then approximated from the infinite-dimensional controllers. It is shown that the finite-dimensional controllers provide robust stabilization in the presence of small time delays in the systems. On the other hand, our approach is to truncate the infinite-dimensional models of the systems and to add feedthrough terms to the truncated models to compensate for the neglected dynamics. The finite-dimensional spatial $\mathcal{H}_\infty$ controllers are then designed based on the corrected finite-dimensional models.

The purpose of the feedthrough term is to significantly reduce the uncertainty associated with the truncated model. It is known that the gain and locations of the in-bandwidth zeros are not accurate because of truncation [5]–[8]. This inaccuracy can have negative effect on the closed-loop stability. To fix this problem, we add a feedthrough term to the truncated model to correct the gain and locations of the zeros as discussed in [5]–[8]. This technique is known in the aeroelasticity literature as the mode-acceleration method [9]. Incorporating the feedthrough term into the truncated (finite dimensional) model reduces the uncertainty associated with the truncation, which is important in ensuring the closed-loop robustness.

To demonstrate our proposed controller, a single input–single output (SISO) spatial $\mathcal{H}_\infty$ controller is designed for a piezoelectric-laminate beam to suppress the vibration of the first six bending modes of the structure. The controller is applied to a real structure, a simply-supported beam with a collocated piezoelectric actuator–sensor pair. Piezoelectric devices have shown promising applications in active vibration control of flexible structures [10]–[14]. The ability of piezoelectric materials to convert mechanical strain into electrical voltage and vice versa allows them to be used as actuators and sensors when placed on flexible structures.

The problem of the $\mathcal{H}_\infty$ control for distributed systems has been addressed in the literature (such as in [2]–[4] and [15]–[17]). In [2]–[4] and [17], the models for the controller design only describe vibrations at one or several locations along the structures, i.e., pointwise models. Thus, the controller is designed based on the information of one or a few locations along the structure. In contrast, the main emphasis of the control-design methodology presented here is to reduce vibration of the structure in a spatial sense. This is done by employing the spatial information embedded within the

Manuscript received December 8, 2000; revised February 13, 2002. This work was supported in part by the Center for Integrated Dynamics and Control and in part by the Australian Research Council under Grant DP 0209396. Recommended by Technical Editor C. H. Menq.

The authors are with the School of Electrical Engineering and Computer Science, University of Newcastle, Callaghan, NSW 2308, Australia (e-mail: dunanth@ee.newcastle.edu.au; reza@ee.newcastle.edu.au).

Publisher Item Identifier 10.1109/TMECH.2002.802727.

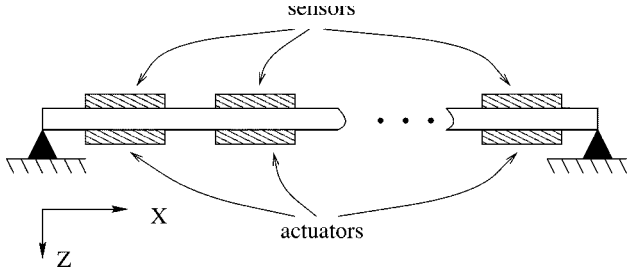

Fig. 1. Simply-supported beam with a number of collocated piezoelectric patches.

models of structures that result from the modal analysis. A further purpose of the paper is to ensure that the developed methodology is implementable on flexible structures. This is demonstrated by implementing a spatial $\mathcal{H}_\infty$ controller on a piezoelectric-laminate beam.

This paper is organized as follows. Section II describes the dynamics of flexible structures such as those with collocated piezoelectric actuator–sensor pairs. Section III briefly describes the notion of spatial norms that are used as performance measures for flexible structures. Section IV deals with the model correction to compensate for the neglected dynamics in the truncated (finite-dimensional) model. Section V describes the concept of spatial $\mathcal{H}_\infty$ control for flexible structures. Section VI discusses the design of a feedback SISO controller for suppressing the vibration of the first six bending modes of a simply-supported piezoelectric-laminate beam. Section VII presents experimental validations on the application of the developed controller to a beam structure. The last section concludes the paper.

II. Models of Flexible Structures

In this section, we briefly explain how a model of a beam with a number of collocated PZT actuator–sensor pairs can be obtained using a modal analysis technique. Interested readers can refer to [11], [12] for more detailed derivations.

Consider a homogeneous Euler–Bernoulli beam with length L, width W, and thickness h as shown in Fig. 1. The piezoelectric actuators and sensors have length L_{px}, width L_{py}, and thickness h_p. In this paper, we assume that $h_p \ll h$, which is true for the patches that are used in our experiments. Thus, the assumption of uniform beam properties can be justified. However, we can also use approximation methods such as the finite-element method to deal with more general nonuniform structures.

Suppose there are M collocated actuator–sensor pairs distributed along the structure. Piezoelectric patches on one side of the beam are used as sensors, while patches on the other side are used as actuators. Voltages that are applied to actuating patches are represented by $V_a(t) = [V_{a1}(t), \ldots, V_{aM}(t)]^T$.

We assume that a model of the structure is obtained via the modal analysis procedure. This procedure requires finding a solution to the partial differential equation (PDE) which describes the dynamics of the composite system. The governing PDE of a flexible beam is as follows [10], [18]:

$$EI\,\frac{\partial^4 z(t,\,x)}{\partial x^4} + \rho A_b\,\frac{\partial^2 z(t,\,x)}{\partial t^2} = \frac{\partial^2 M_{px}(t,\,x)}{\partial x^2} \qquad (1)$$

where the beam transverse deflection at point x and at time t is denoted by $z(t,\,x)$. Also, ρ and A_b represent the density and the cross-sectional area of the beam, while E and I are the Young's Modulus and the moment of inertia about the neutral axis of the beam, respectively. The right-hand-side term represents the forcing function produced by the piezoelectric actuator. In this case, M_{px} is the forcing moment acting on the beam.

The PDE can be solved independently for each mode by using the orthogonality properties of its eigenfunctions W_k which are as follows for the case of a uniform beam:

$$\int_0^L W_k(x)W_p(x)\,dx = \delta_{kp} \qquad (2)$$

$$\int_0^L \frac{EI}{\rho A_b}\,\frac{d^4 W_k}{dx^4}\,W_p\,dx = \omega_k^2 \delta_{kp} \qquad (3)$$

where ω_k describes the natural frequency of the beam at mode k. Here, δ_{kp} is Kronecker's delta function, that is, $\delta_{kp} = 0$ for all $k \neq p$, and equals one if $k = p$.

The multiple-input, infinite-output (MIIO) transfer function from the applied actuator-voltages $V_a(s)$ to the transverse structural deflection $z(s,\,x)$ at location x is

$$G(s,\,x) = P\sum_{k=1}^{\infty} \frac{W_k(x)\overline{\Psi}_k^T}{s^2 + 2\zeta_k\omega_k s + \omega_k^2} \qquad (4)$$

where $\overline{\Psi}_k = [\Psi_{k1}, \ldots, \Psi_{kM}]^T$ and the mode number is denoted by k. Ψ_{ki} is a function of the location of the ith piezoelectric actuator–sensor pair and the eigenfunction $W_k(x)$ (see [14], [19], [20]). The damping ratio is denoted by ζ_k and P, respectively, is a constant that is dependent on the properties of the structure and the piezoceramic patches.

Such models have the interesting property that they describe spatial and spectral properties of the system. The spatial information of these models can then be used to design controllers, which guarantee a certain level of damping for the entire structure.

Furthermore, the multiple input–multiple output (MIMO) transfer function of the flexible structure with piezoelectric actuator–sensor (collocated) pairs can be determined in a similar manner. The transfer function from the applied actuator-voltages $V_a(s)$ to the induced voltages at the sensor $V_s(s) = [V_{s1}(s), \ldots, V_{sM}(s)]^T$ is

$$G_{Vs}(s) = P_{Vs}\sum_{k=1}^{\infty} \frac{\overline{\Psi}_k\overline{\Psi}_k^T}{s^2 + 2\zeta_k\omega_k s + \omega_k^2} \qquad (5)$$

where $P_{Vs} = \Upsilon P > 0$ is a constant based on the properties of the structure and the piezoceramic patches.

III. Spatial Norms

This section presents an overview of the spatial norms of signals and systems. For a more detailed review of this concept, the reader is referred to [8]. Consider the transfer function $G(s,\,x)$, where $x \in X$, which maps an input signal $w(t) \in \mathbf{R}^m$ to the output signal $z(t,\,x) \in \mathbf{R} \times X$ (see Fig. 2). Here, $z(t,\,x)$ is spatially distributed over the set X.

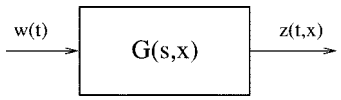

Fig. 2. System $G(s,\ x)$.

The spatial $\mathcal{H}_2$ norm of the signal $z(t,\ x)$ is defined as

$$\langle\langle z\rangle\rangle_2^2 = \int_0^\infty \int_X z(t,\ x)^T z(t,\ x)\, dx\, dt. \tag{6}$$

The spatial $\mathcal{H}_2$ norm of the signal z can be interpreted as the total energy of the signal $z(t,\ x)$. Now, let $\mathcal{G}$ be the linear operator which maps the inputs of $G(s,\ x)$ to its outputs. The spatial induced norm of $\mathcal{G}$ is defined as (see [8])

$$\langle\langle \mathcal{G}\rangle\rangle^2 = \sup_{0\neq w\in\mathcal{L}_2[0,\,\infty)} \frac{\langle\langle z\rangle\rangle_2^2}{||w||_2^2} \tag{7}$$

where $||w||_2^2 = \int_0^\infty w(t)^T w(t)\, dt$.

Moreover, following [8], the spatial $\mathcal{H}_\infty$ norm of $G(s,\ x)$ is defined as

$$\langle\langle G\rangle\rangle_\infty^2 = \sup_{\omega\in\mathbf{R}} \lambda_{\max}\left(\int_X G(j\omega,\ x)^* G(j\omega,\ x)\, dx\right) \tag{8}$$

where $\lambda_{\max}(F)$ represents the maximum eigenvalue of the matrix F.

Reference [8, Theorem (3.1)] gives a representation of the spatial $\mathcal{H}_\infty$ norm of $G(s,\ x)$ in terms of total energy of $z(t,\ x)$ and energy of the input signal $w(t)$. The theorem states that

$$\langle\langle \mathcal{G}\rangle\rangle = \langle\langle G\rangle\rangle_\infty. \tag{9}$$

It is possible to add spatial weights to all of the above definitions, to emphasize the regions that are of more importance. This issue will be further explained in Section V.

IV. Model Correction

In practice, dynamical models of a flexible structure as described in (4) and (5) can be truncated to represent the system with a finite-dimensional model. The model can be truncated so to include only the modes within the frequency bandwidth of interest. However, the neglected dynamics associated with truncation of the model produces additional error in the gain and locations of the in-bandwidth zeros. This is due to the fact that the contribution of the out-of-bandwidth modes is ignored in the truncation. As a consequence, the neglected dynamics can be detrimental to the robustness of the closed-loop system.

One way to improve the truncated model dynamics is to include a feedthrough term to correct the gain and locations of the in-bandwidth zeros. This technique is known in the aeroelasticity literature as the mode-acceleration method [9] and has been revisited in [5]–[8]. Adding a feedthrough term to the truncated (finite dimensional) model compensates for the neglected dynamics in the model, which is important in ensuring the closed-loop stability.

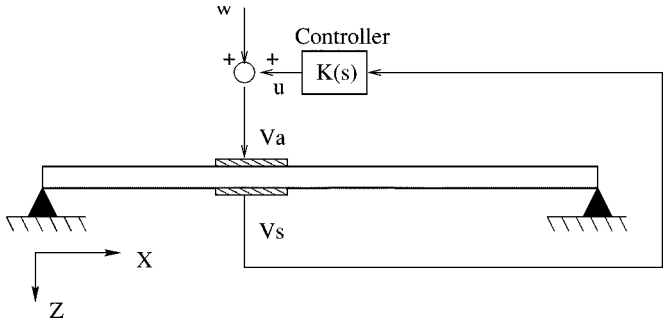

Fig. 3. Spatial $\mathcal{H}_\infty$ control of a flexible beam.

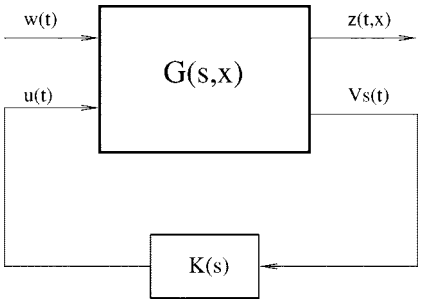

Fig. 4. Spatial $\mathcal{H}_\infty$ control problem.

The infinite-dimensional model of the collocated system in (5) can be approximated as

$$G_{Vs}^N(s) = P_{Vs}\sum_{k=1}^{N} \frac{\overline{\Psi}_k \overline{\Psi}_k^T}{s^2 + 2\zeta_k\omega_k s + \omega_k^2} + K_{Vs} \tag{10}$$

where N is the number of modes included in the model, and K_{Vs} is a $M \times M$ matrix added to compensate for the neglected dynamics. For a general multivariable system, K_{Vs} can be found using the method proposed in [7]. For a SISO system, K_{Vs} will be a scalar.

Similarly, we describe the approximate spatial transfer function of $G(s,\ x)$ in (4) by

$$G^N(s,\ x) = P\sum_{k=1}^{N} \frac{W_k(x)\overline{\Psi}_k^T}{s^2 + 2\zeta_k\omega_k s + \omega_k^2} + K(x) \tag{11}$$

where $K(x)$ is a $1 \times M$ vector. $K(x)$ is a function of the spatial variable, x. It has to be estimated from the modal model of the system.

One technique that can be used is to find the feedthrough term that minimizes the weighted spatial $\mathcal{H}_\infty$ norm of the error between the infinite dimensional and truncated models is presented in [8]. The term $K(x)$ is determined such that the following cost function is minimized:

$$J = \langle\langle W_c(s,\ x)(G(s,\ x) - G^N(s,\ x))\rangle\rangle_\infty^2. \tag{12}$$

Here, $W_c(s,\ x)$ is an ideal low-pass weighting function distributed spatially over X with its cutoff frequency ω_c chosen to lie within the interval $\omega_c \in (\omega_N,\ \omega_{N+1})$.

The cost function (12) is minimized by setting [8]

$$K(x) = \sum_{k=N+1}^{\infty} K_k^{opt} W_k(x) \tag{13}$$

Fig. 5. Piezoelectric-laminate beam.

where

$$K_k^{opt} = \frac{1}{2}\left(\frac{1}{\omega_k^2} + \frac{1}{\omega_k^2 - \omega_c^2}\right) P\overline{\Psi}_k^T. \tag{14}$$

Note, that in practice we can only include a finite number of modes to calculate the feedthrough term, $K(x)$. So, $K(x)$ in (13) is calculated from $k = N+1$ to $N_{\max}$ with $N_{\max}$ is chosen so that the neglected dynamics in the model can be compensated sufficiently. Naturally, the larger $N_{\max}$, the smaller the uncertainty will be. However, choosing a large enough $N_{\max}$ is quite reasonable as its effect diminishes when $N_{\max} \to \infty$ since the contribution of higher frequency modes is decreasing (see [6]). Furthermore, since the calculation of the feedthrough term in (13) is straightforward, there is no restriction on how many high frequency (out-of-bandwidth) modes can be included in the calculation.

V. Spatial $\mathcal{H}_\infty$ Control of a Piezoelectric-Laminate Beam

This section is concerned with the problem of spatial $\mathcal{H}_\infty$ control for flexible structures. Consider a typical disturbance rejection problem for a flexible structure such as the one shown in Fig. 3. The system consists of only one piezoelectric actuator–sensor pair for the sake of clarity. Here, the purpose of the controller is to reduce the effect of disturbance $w(t)$ on the entire structure, using piezoelectric actuators and sensors. The concept of spatial $\mathcal{H}_\infty$ control was introduced in [1] to address problems of this nature.

A spatially-distributed linear time-invariant dynamical system such as the beam in Fig. 3 can be defined in its state-space form as

$$\begin{aligned} \dot{\overline{x}}(t) &= A\overline{x}(t) + B_1 w(t) + B_2 u(t) \\ z(t,\, x) &= C_1(x)\overline{x}(t) + D_{11}(x)w(t) + D_{12}(x)u(t) \\ V_s(t) &= C_2\overline{x}(t) + D_{21}w(t) + D_{22}u(t) \end{aligned} \tag{15}$$

where $\overline{x} \in \mathbf{R}^n$ is the state, $w \in \mathbf{R}$ is the disturbance input, $u \in \mathbf{R}$ is the control input, z is the performance output, $V_s \in \mathbf{R}$ is the measured output. For a flexible structure, $z(t,\, x)$ represents the spatial displacement at time t, where $x \in X$.

The system matrices in (15) can be obtained from transfer functions (10) and (11). Note, that for the system shown in Fig. 3, $D_{22} = D_{21}$ in (15) is the feedthrough term K_{Vs} described in (10), while $D_{11}(x) = D_{12}(x)$ is $K(x)$ in (13). Moreover, $B_1 = B_2$ since disturbance is assumed to enter the system through the actuator.

TABLE I
Properties of PIC151 Piezoceramics

Piezoceramic Young's Modulus, E_p	6.70×10^{10} N/m^2
Charge constant, d_{31}	-2.10×10^{-10} m/V
Voltage constant, g_{31}	-1.15×10^{-2} Vm/N
Capacitance, C	1.05×10^{-7} F
Electromechanical coupling factor, k_{31}	0.34

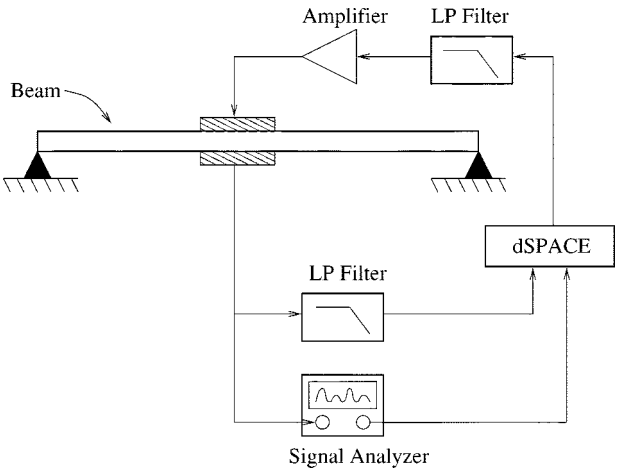

Fig. 6. Experimental setup.

The spatial $\mathcal{H}_\infty$ control problem is to design a controller

$$\begin{aligned} \dot{x}_k(t) &= A_k x_k(t) + B_k V_s(t) \\ u(t) &= C_k x_k(t) + D_k V_s(t) \end{aligned} \tag{16}$$

such that the closed-loop system satisfies

$$\inf_{K \in U} \sup_{w \in \mathcal{L}_2[0,\,\infty)} J_\infty < \gamma^2 \tag{17}$$

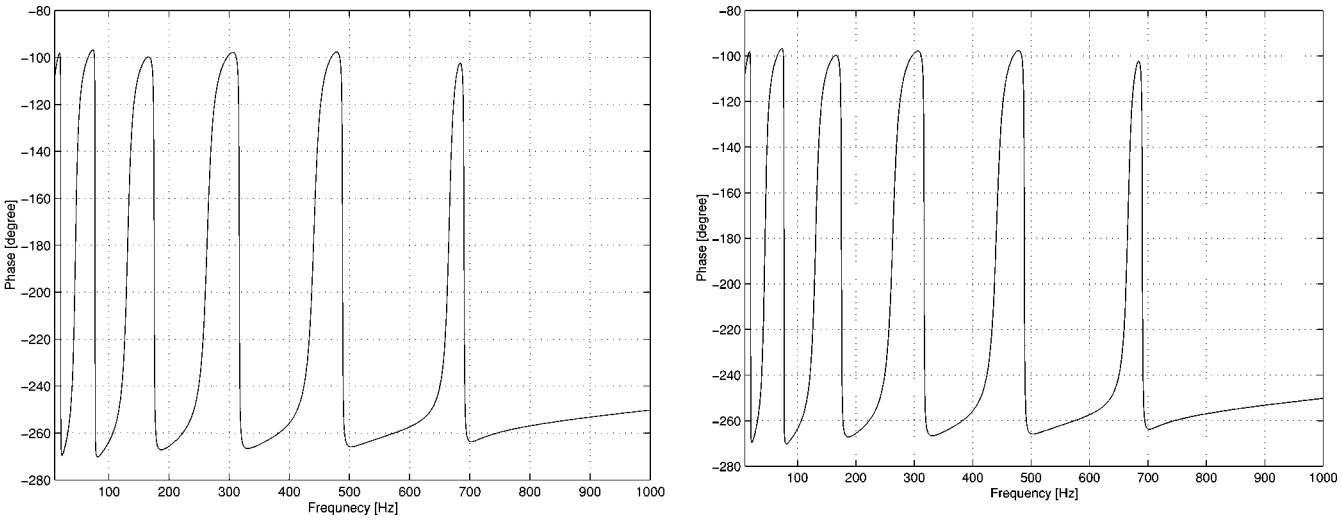

(a) (b)

Fig. 7. Frequency response of the controller (input voltage to output voltage [V/V]).

where U is the set of all stabilizing controllers and

$$J_\infty = \frac{\int_0^\infty \int_X z(t,x)^T Q(x) z(t,x)\, dx\, dt}{\int_0^\infty w(t)^T w(t)\, dt}. \tag{18}$$

Here, $Q(x)$ is a spatial-weighting function. The purpose of $Q(x)$ is to emphasize the region where the vibration is to be damped more heavily. The numerator in (18) is the weighted spatial $\mathcal{H}_2$ norm of $z(t,x)$ [21], [22]. Therefore, J_∞ can be interpreted as the ratio of the spatial energy of the output of the system to the energy of its input. The control problem is depicted in Fig. 4.

It can be shown by the method in [1] that the above problem is equivalent to a standard $\mathcal{H}_\infty$ control problem for the following system:

$$\begin{aligned} \dot{\overline{x}}(t) &= A\overline{x}(t) + B_1 w(t) + B_2 u(t) \\ \tilde{z}(t) &= \Pi\overline{x}(t) + \Theta w(t) + \Theta u(t) \\ V_s(t) &= C_2\overline{x}(t) + D_{21} w(t) + D_{22} u(t) \end{aligned} \tag{19}$$

where $D_{21} = D_{22}$ and $[\Pi \quad \Theta \quad \Theta] = \Gamma$. Here, Γ is any matrix that satisfies

$$\Gamma^T\Gamma = \int_X \begin{bmatrix} C_1(x)^T \\ D_{11}(x)^T \\ D_{12}(x)^T \end{bmatrix} Q(x)[C_1(x) D_{11}(x) D_{12}(x)]\, dx \tag{20}$$

where $D_{11}(x) = D_{12}(x)$. Hence, the system in (19) can be solved using a standard $\mathcal{H}_\infty$ control technique [23], [24]. The spatial $\mathcal{H}_\infty$ controller can be regarded as a controller that reduces structural vibration in a spatially averaged sense. The resonant peaks will be particularly targeted by this controller, which is desirable for our purpose of minimizing structural vibration.

It can be observed that the $\mathcal{H}_\infty$ control problem associated with the system described in (19) is nonsingular. This is due to the existence of feedthrough terms from the disturbance to the measured output and from the control signal to the performance output. Had we not corrected the location of in-bandwidth zeros, the resulting $\mathcal{H}_\infty$ control problem would have been singular.

Designing a $\mathcal{H}_\infty$ controller for the system (19) may result in a very high-gain controller. This could be attributed to the fact that the term Θ in (19) does not represent a physical weight on the control signal. Rather, it represents the effect of truncated modes on the in-bandwidth dynamics of the system, which is important in ensuring the robustness of the closed-loop system. This problem can be fixed by introducing a weight on the control signal. This can be achieved by rewriting (19) as

$$\begin{aligned} \dot{\overline{x}}(t) &= A\overline{x}(t) + B_1 w(t) + B_2 u(t) \\ \hat{z}(t) &= \begin{bmatrix} \Pi \\ 0 \end{bmatrix} \overline{x}(t) + \begin{bmatrix} \Theta \\ 0 \end{bmatrix} w(t) + \begin{bmatrix} \Theta \\ R \end{bmatrix} u(t) \\ V_s(t) &= C_2\overline{x}(t) + D_{21} w(t) + D_{22} u(t) \end{aligned} \tag{21}$$

where R is a weighting matrix with compatible dimensions.

What makes this system different from (19) is the existence of matrix R in the error output $\hat{z}$. The matrix R serves as a weighting matrix to balance the controller effort with respect to the degree of vibration reduction that can be achieved. This can be shown to be equivalent to adding a term, $\int_0^\infty u(t)^T R^T R u(t)\, dt$, to the numerator of the cost function, J_∞ in (18). Setting R with smaller elements might lead to higher vibration reduction but at the expense of a higher controller gain. In practice, one has to make a compromise between the level of vibration reduction and controller gain by choosing a suitable R.

To this end, it should be clear that the model correction performed in the previous section is instrumental in ensuring robustness of the closed-loop system. One approach to guaranteeing closed-loop robustness is to model the truncated dynamics as an uncertainty block as in [25], [26]. By adding an appropriate feedthrough term, however, the uncertainty associated with the truncated model is significantly reduced. This is in contrast to the approach in [2]–[4] where an infinite-dimensional controller is obtained from an infinite-dimensional model and a finite-dimensional controller is approximated afterwards.

The choice for N is a direct result of the bandwidth that is of control significance. If one is interested in controlling the

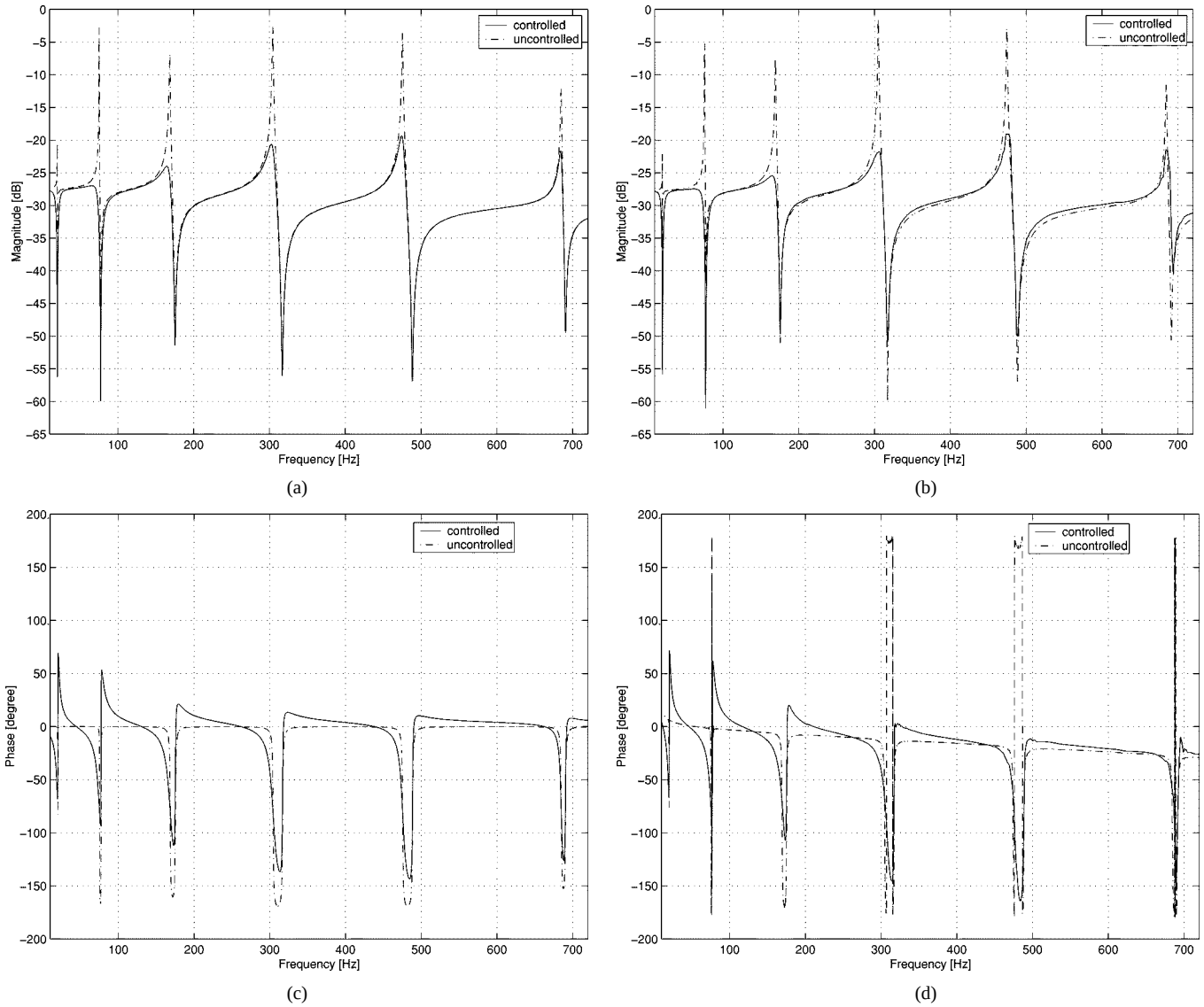

Fig. 8. Simulation and experimental frequency responses (actuator voltage to sensor voltage [V/V]).

first six modes, then it is sufficient to consider only the first six modes in the truncated model, i.e., $N = 6$. Since the dimensions of the plant and optimal controller are similar, one would obtain a 12th-order controller for $N = 6$. This is advantageous since the controller has a minimal order necessary to control the first six modes.

The main purpose of this work is to design controllers that guarantee vibration reduction in a spatial $\mathcal{H}_\infty$ sense. This is in contrast to the previous works that deal with pointwise models [2]–[4], [17]. One possibility in dealing with the robustness issue is to model the residual uncertainty as a spatially distributed uncertain block. The methodology presented here can then be extended to explicitly allow for this uncertainty description. This work however, is relegated to the future.

VI. Controller Design

In this section, effectiveness of the spatial $\mathcal{H}_\infty$ control method will be demonstrated on a laboratory scale apparatus. A simply-supported flexible beam—such as the one shown in Fig. 1—with a collocated piezoelectric actuator–sensor pair attached to it is used in the experiments. The apparatus is shown in Fig. 5. The structure consists of a 60-cm long uniform aluminum beam of a rectangular cross section (50 mm $\times$ 3 mm). The beam is pinned at both ends. A pair of piezoelectric-ceramic elements are attached symmetrically to either side of the beam, 50 mm away from one end of the beam. The piezoceramic elements used in our experiment are PIC151 patches. These patches are 25–mm wide, 70-mm long and 0.25-mm thick. The physical parameters of PIC151 are given in Table I. A model of the composite structure is obtained via modal analysis. We use the equivalent standard $\mathcal{H}_\infty$ control problem described in (21) for our spatial $\mathcal{H}_\infty$ controller. Here, V_s is the output voltage from the piezoelectric sensor, while u is the control input voltage from the controller.

Here, we wish to control only the first six bending modes of the beam via a SISO controller. Hence, the model is truncated to include only the first six modes. The $\mathcal{H}_\infty$ control design procedure will then produce a 12th-order controller. The effect of out-of-bandwidth modes has to be taken into consideration

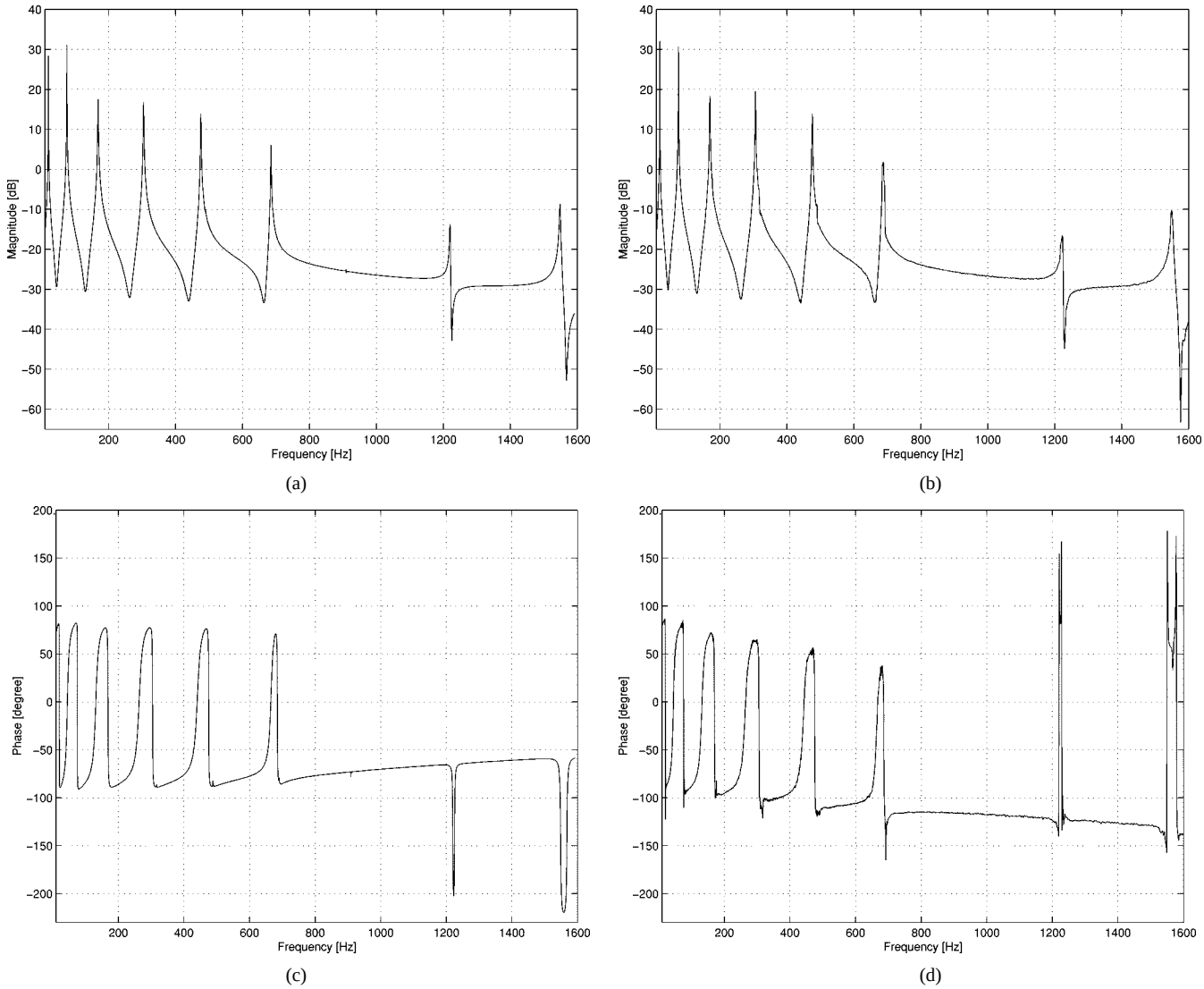

Fig. 9. Loop gain [V/V]: simulation and experiment.

to compensate for the neglected dynamics in the truncated model as discussed in Section IV. Based on the experimental frequency-response data from actuator voltage to sensor voltage, the feedthrough term in (10), $D_{21} = D_{22} = K_{Vs}$, is found to be 0.033 if the first six modes are considered in the model (see also [27]).

Since the disturbance is assumed to enter the system through the same channel as the controller, the SISO transfer functions from w and u to the transverse deflection of the beam $z(t, x)$ are the same, i.e., $G^N(s, x)$. Incorporating (13) and (14) in (11), we have

$$G^N(s, x) = P\sum_{k=1}^{N} \frac{W_k(x)\overline{\Psi}_k}{s^2 + 2\zeta_k\omega_k s + \omega_k^2} + \sum_{k=N+1}^{N_{\max}} K_k^{opt} W_k(x). \tag{22}$$

The feedthrough term is calculated by considering modes $N+1$ to $N_{\max} = 200$ to obtain a reasonable spatial approximation to the feedthrough term. A larger $N_{\max}$ can be used instead, but the value of the feedthrough term would not change significantly because of the reason described in Section IV. Similarly, the SISO transfer functions from w and u to the collocated sensor voltage V_s are denoted by $G_{Vs}^N(s)$ (10)

$$G_{Vs}^N(s) = P_{V_s}\sum_{k=1}^{N} \frac{\overline{\Psi}_k^2}{s^2 + 2\zeta_k\omega_k s + \omega_k^2} + K_{Vs}. \tag{23}$$

The state-space model of the spatial $\mathcal{H}_\infty$ control problem can be defined as in (15), with

$$A = \begin{bmatrix} 0_{N\times N} & I_{N\times N} \\ A_{21} & A_{22} \end{bmatrix}$$

where

$$A_{21} = -diag(\omega_1^2, \ldots, \omega_N^2)$$
$$A_{22} = -2diag(\zeta_1\omega_1, \ldots, \zeta_N\omega_N)$$

and

$$B_1 = B_2 = P[0 \quad \cdots \quad 0 \quad \Psi_{11} \quad \cdots \quad \Psi_{N1}]^T$$
$$C_1(x) = [W_1(x) \quad \cdots \quad W_N(x) \quad 0 \quad \cdots \quad 0]$$
$$C_2 = \Upsilon[\Psi_{11} \quad \cdots \quad \Psi_{N1} \quad 0 \quad \cdots \quad 0]$$

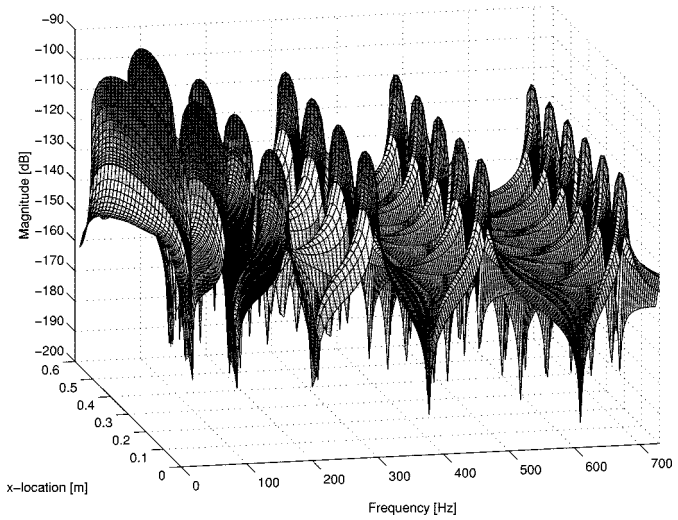

Fig. 10. Simulation spatial frequency response: actuator voltage—beam deflection (open loop) [m/V].

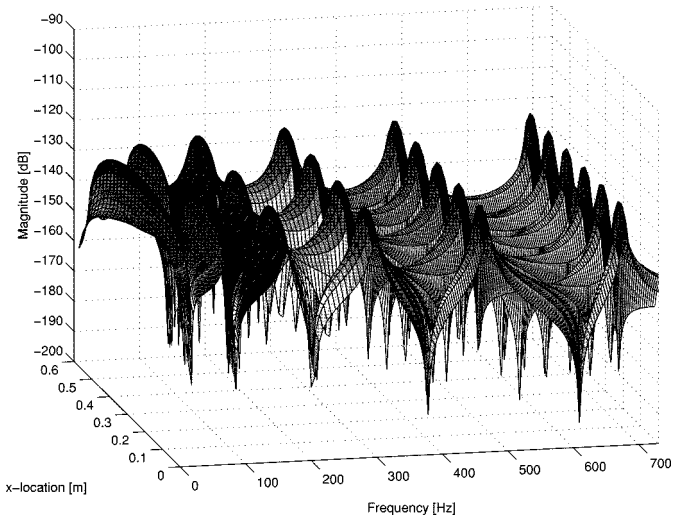

Fig. 11. Simulation spatial frequency response: actuator voltage—beam deflection (closed loop) [m/V].

$$D_{11}(x) = D_{12}(x) = \sum_{k=N+1}^{N_{\max}} K_k^{opt} W_k(x)$$
$$D_{21} = D_{22} = K_{Vs}. \tag{24}$$

The spatial weighting function $Q(x)$ is set equal to one, which means that all points along the beam are weighted equally. Based on (20), we can obtain the error output in (21), $\hat{z}$, using the orthogonality property in (2), with Π and Θ as follows:

$$\Pi = \begin{bmatrix} I_{N\times N} & 0_{N\times N} \\ 0_{N\times N} & 0_{N\times N} \\ 0_{1\times N} & 0_{1\times N} \end{bmatrix}$$
$$\Theta = \begin{bmatrix} 0_{2N\times 1} \\ \left(\sum_{k=N+1}^{N_{\max}} (K_k^{opt})^2 \right)^{1/2} \end{bmatrix}. \tag{25}$$

The scalar weighting factor R can then be determined to find a controller with sufficient damping properties and robustness. Matlab μ-Analysis and Synthesis Toolbox was used to calculate our spatial $\mathcal{H}_\infty$ controller based on the system in (21) via a state-space approach.

VII. Experimental Validations

The experiment was set in the Laboratory for Dynamics and Control of Smart Structures at the University of Newcastle, Australia. The experimental setup is depicted in Fig. 6. The controller was implemented using a dSpace DS1103 rapid prototyping Controller Board together with the MATLAB-Simulink[1] software. The sampling frequency was set at 20 KHz. The cutoff frequencies of the two low-pass filters were set at 3 KHz. A high-voltage amplifier, capable of driving highly capacitive loads, was used to supply necessary voltage for the actuating piezoelectric patch. An HP89410A Dynamic

[1]MATLAB-Simulink is a registered trademark of The MathWorks, Natick, MA.

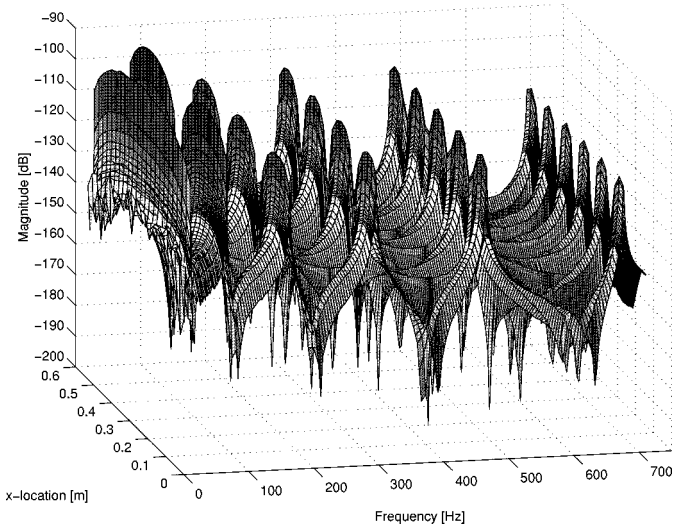

Fig. 12. Experimental spatial frequency response: actuator voltage—beam deflection (open loop) [m/V].

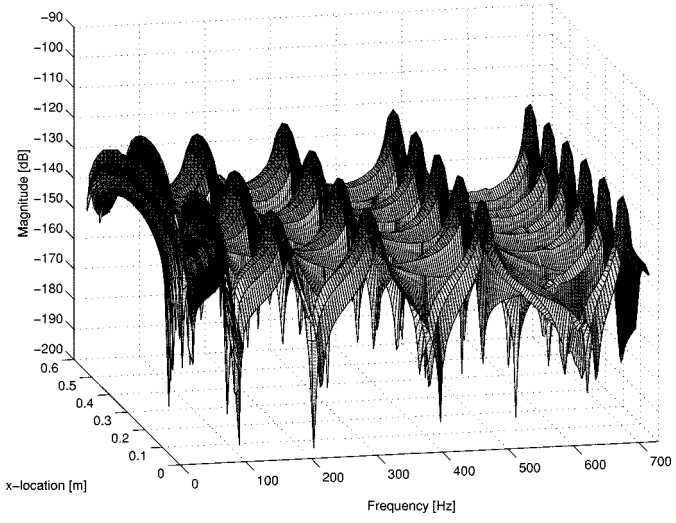

Fig. 13. Experimental spatial frequency response: actuator voltage—beam deflection (closed loop) [m/V].

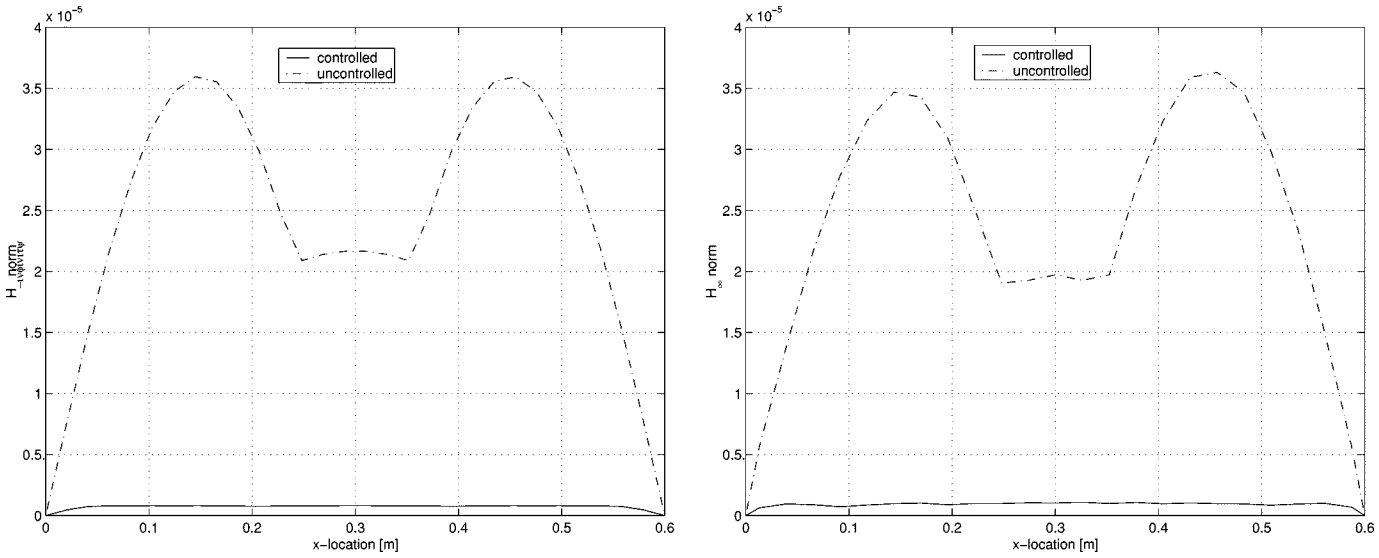

Fig. 14. Simulation and experimental $\mathcal{H}_\infty$ norm plot—spatial control.

Signal Analyzer and a Polytec PSV-300 Laser Doppler Scanning Vibrometer were used to obtain frequency responses of the piezoelectric-laminate beam. Important parameters of the beam, such as resonant frequencies and damping ratios, were obtained from the experiment and were used to correct our model.

Our simulation and experimental results are presented in the following. The frequency response of the controller is shown in Fig. 7. It can be observed that the controller has a resonant nature. This is expected and can be attributed to the highly resonant nature of the beam. That is, the controller tries to apply a high gain at each resonant frequency. Fig. 8 compares frequency responses of the open-loop and closed-loop systems (actuator voltage to sensor voltage) for both simulation and experimental results. It can be observed that the performance of the controller applied to the real system is as expected. The comparison between simulation and experimental frequency responses shows that the approach in incorporating a feedthrough term into the truncated model to compensate for the neglected dynamics works very well. The resonant responses of modes 1–6 of the system have been reduced considerably once the controller was introduced.

A comparison of the loop gain up to 1.6 KHz from simulation and experiment is shown in Fig. 9. Our simulation gives a gain margin of 11.3 dB at 1.55 KHz and a phase margin of 89.0° at 79.3 Hz. The experiment gives a gain margin of 10.7 dB at 1.55 KHz, and a phase margin of 87.1° at 79.6 Hz. Some reduction of the stability margin in the real system is expected because of the phase delay associated with the digital controller and filters used in the experiment as seen in Fig. 9. Moreover, there may be a slight difference between our model and the real plant, i.e., modal damping ratios and resonant frequencies. This can contribute to the loss of robustness.

Figs. 10 and 11 show the simulated spatial frequency responses of the uncontrolled and controlled beam, respectively. Here, x is measured from one end of the beam, which is closer to the patches, while the frequency response is in terms of the beam's transverse displacement (displacement in z axis). It is clear that vibration of the entire beam due to the first six bending modes has been reduced by the action of the controller.

Next, a Polytec PSV-300 Laser Scanning Vibrometer was used to obtain the frequency response of the beam's vibration at a number of points on the surface. The results allow us to plot the spatial frequency responses of the uncontrolled and controlled beam using the experimental results as shown in Figs. 12 and 13. It can be observed that the resonant responses of modes 1–6 have been reduced over the entire beam due to the controller action, which is as expected from the simulation (compare with Figs. 10 and 11). The resonant responses of modes 1–6 have been reduced by approximately 27, 30, 19.5, 19.5, 15.5, and 8 dB, respectively, over the entire beam. Thus, our spatial $\mathcal{H}_\infty$ controller minimizes resonant responses of selected vibration modes over the entire structure, which is desirable for vibration suppression purposes.

To demonstrate the controller's effect on the spatial $\mathcal{H}_\infty$ norm of the system, we have plotted the pointwise $\mathcal{H}_\infty$ norm of the controlled and uncontrolled beam as a function of x in Fig. 14. The figures show that the experimental results are very similar to the simulations. Furthermore, they clearly show the effect of our spatial $\mathcal{H}_\infty$ controller in reducing the vibration of the beam. It is obvious that the $\mathcal{H}_\infty$ norm of the entire beam has been reduced by the action of the controller in a uniform manner. The largest $\mathcal{H}_\infty$ norm of the uncontrolled beam has been reduced by approximately 97%, from 3.6×10^{-5} to 1.1×10^{-6}.

The effectiveness of the controller in minimizing beam's vibration in time domain can be seen in Fig. 15. A step disturbance signal with amplitude of 100 V was applied through the piezoelectric actuator. The velocity response of the beam, at a point 80 mm away from one end of the beam, was observed using the PSV Laser Vibrometer. The velocity response was filtered by a bandpass filter from 10 to 750 Hz. The settling time of the velocity response has been reduced considerably.

To show the advantage of the spatial $\mathcal{H}_\infty$ control over the pointwise $\mathcal{H}_\infty$ control, we performed the following experiment.

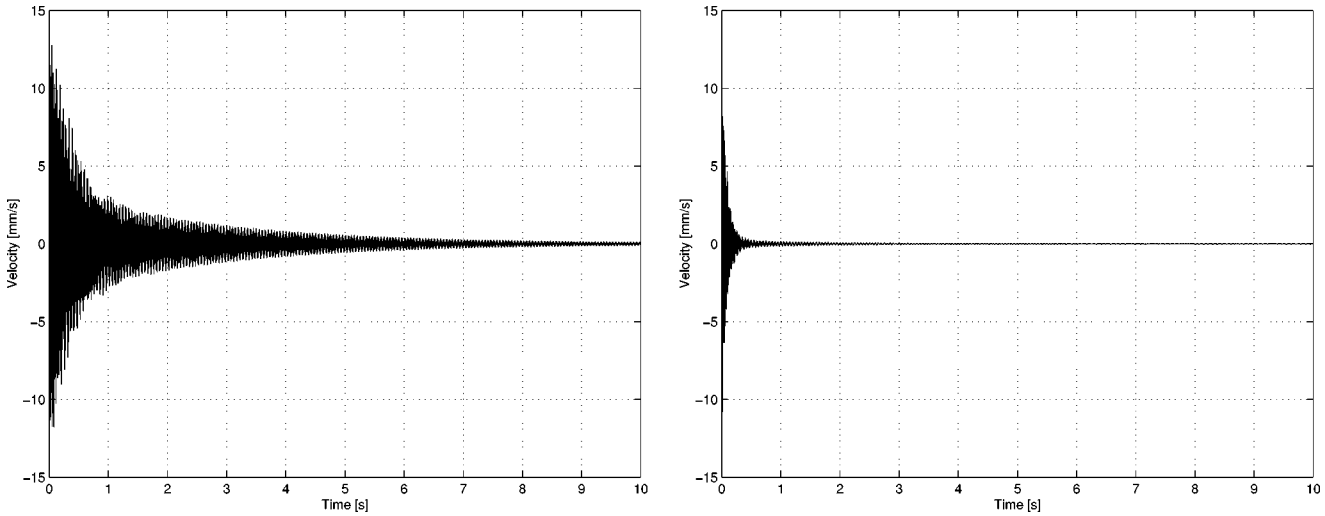

Fig. 15. Vibration at a point 80 mm away from one end of the beam.

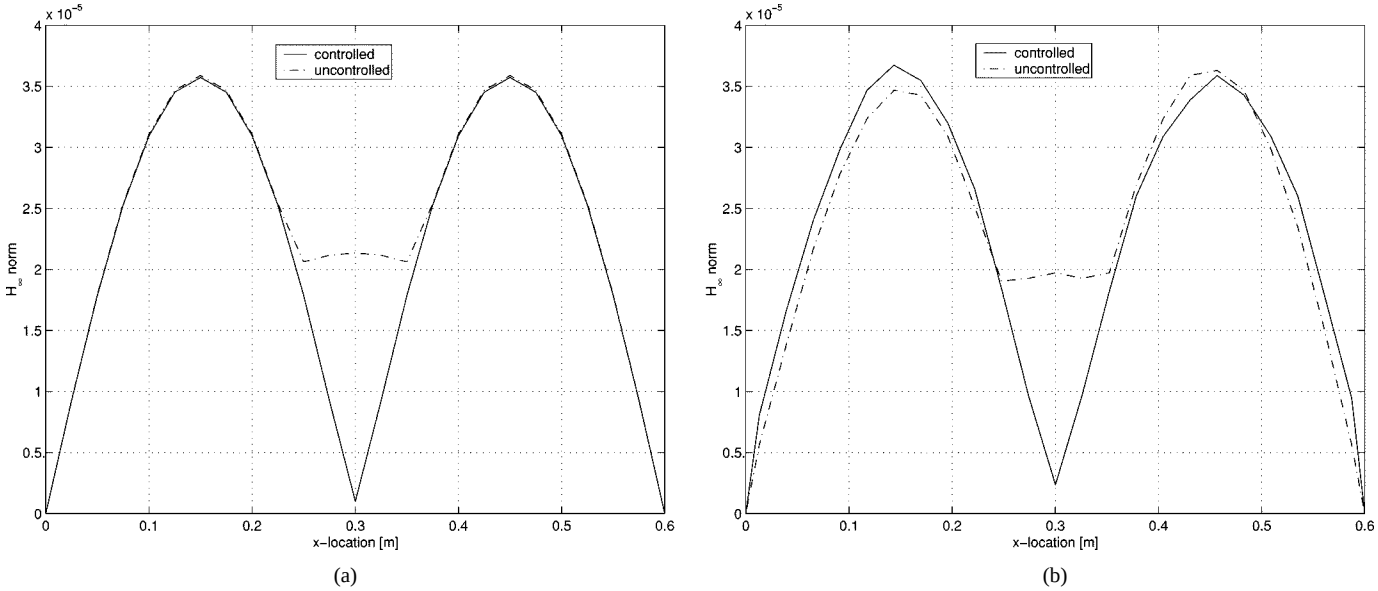

Fig. 16. Simulation and experimental $\mathcal{H}_\infty$ norm plot—pointwise control.

A pointwise $\mathcal{H}_\infty$ controller was designed to minimize the $\mathcal{H}_\infty$ norm of the closed-loop transfer function from the disturbance w to the deflection at the middle of the beam, i.e., $x = 0.3$ m. The controller had a gain margin of 14.3 dB and a phase margin of 77.9°. It was implemented on the beam using the setup in Fig. 6. In Fig. 16, we have plotted $\mathcal{H}_\infty$ norm of the controlled and uncontrolled beam as a function of x.

Fig. 16 shows the effectiveness of the pointwise control in local reduction of the $\mathcal{H}_\infty$ norm at and around $x = 0.3$ m. This is not surprising as the only purpose of the controller is to minimize vibration at $x = 0.3$ m. In fact, the pointwise controller only suppresses the odd-numbered modes since $x = 0.3$ m is a node for even-numbered modes. Comparing Figs. 14 and 16, it can be concluded that the spatial $\mathcal{H}_\infty$ controller has an advantage over the pointwise $\mathcal{H}_\infty$ controller as it minimizes the vibration throughout the entire structure.

VIII. Conclusion

A spatial $\mathcal{H}_\infty$ controller was designed and implemented on a piezoelectric-laminate beam. A feedthrough term was added to correct the gain and locations of in-bandwidth zeros of the truncated (finite dimensional) model. Thus, the neglected dynamics in the model can be compensated. This model correction is instrumental in ensuring the robustness of the closed-loop system. It was observed that such a controller resulted in suppression of the transverse deflection of the entire structure by minimizing the spatial $\mathcal{H}_\infty$ norm of the closed-loop system. The controller was obtained by solving a standard $\mathcal{H}_\infty$ control problem for a finite-dimensional system. A number of experiments were performed, which demonstrated the effectiveness of the developed controller in reducing the structural vibrations on a piezoelectric-laminate beam. It was shown that the spatial $\mathcal{H}_\infty$ controller

had an advantage over the pointwise $\mathcal{H}_\infty$ control in minimizing structural vibration of the entire structure. The application of this spatial $\mathcal{H}_\infty$ control is not confined to a piezoelectric-laminate beam. It may be applied to more general vibration suppression problems.

REFERENCES

[1] S. O. R. Moheimani, H. R. Pota, and I. R. Petersen, "Broadband disturbance attenuation over an entire beam," in *Proc. Eur. Control Conf.*, Brussels, Belgium, July 1997.

[2] K. Lenz, H. Özbay, A. Tannenbaum, J. Turi, and B. Morton, "Frequency domain analysis and robust control design for an ideal flexible beam," *Automatica*, vol. 27, no. 6, pp. 947–961, 1991.

[3] ——, "Robust control design for a flexible beam using a distributed-parameter $\mathcal{H}\infty$-method," in *Proc. 28th IEEE Conf. Decision and Control*, 1989, pp. 2674–2678.

[4] K. Lenz and H. Özbay, "Analysis and robust control techniques for an ideal flexible beam," *Control Dyn. Syst.*, vol. 57, pp. 369–421, 1993.

[5] R. L. Clark, "Accounting for out-of-bandwidth modes in the assumed modes approach: Implications on colocated output feedback control," *Trans. ASME, J. Dyn. Syst., Meas., Control*, vol. 119, pp. 390–395, Sept. 1997.

[6] S. O. R. Moheimani, "Minimizing the effect of out-of-bandwidth dynamics in the models of reverberant systems that arise in modal analysis: Implications on spatial $\mathcal{H}_\infty$ control," *Automatica*, vol. 36, pp. 1023–1031, 2000.

[7] ——, "Minimizing the effect of out of bandwidth modes in truncated structure models," *Trans. ASME J. Dyn. Syst., Meas., Control*, vol. 122, pp. 237–239, March 2000.

[8] S. O. R. Moheimani and W. P. Heath, "Model correction for a class of spatio–temporal systems," in *Proc. American Control Conf.*, Chicago, IL, June 2000, pp. 3768–3772.

[9] R. L. Bisplinghoff and H. Ashley, *Principles of Aeroelasticity*. New York: Dover, 1975.

[10] R. L. Clark, W. R. Saunders, and G. P. Gibbs, *Adaptive Structures: Dynamics and Control*. New York: Wiley, 1998.

[11] E. K. Dimitriadis, C. R. Fuller, and C. A. Rogers, "Piezoelectric actuators for distributed vibration excitation of thin plates," *Trans. ASME J. Vib. Acoust. Stress Reliab. Des.*, vol. 113, pp. 100–107, Jan. 1991.

[12] C. R. Fuller, S. J. Elliot, and P. A. Nelson, *Active Control of Vibration*. New York: Academic, 1996.

[13] H. T. Banks, R. C. Smith, and Y. Wang, *Smart Material Structures: Modeling, Estimation and Control*. New York/Paris: Wiley/Masson, 1996.

[14] H. R. Pota and T. E. Alberts, "Multivariable transfer functions for a slewing piezoelectric laminate beam," *Trans. ASME J. Dyn. Syst., Meas., Control*, vol. 117, pp. 352–359, Sept. 1995.

[15] H. Özbay and A. Tannenbaum, "A skew toeplitz approach to the $\mathcal{H}\infty$-optimal control of multivariable distributed systems," *SIAM J. Control Optim.*, vol. 28, no. 3, pp. 653–670, 1990.

[16] ——, "On the structure of suboptimal $\mathcal{H}\infty$ controllers in the sensitivity minimization problem for distributed stable systems," *Automatica*, vol. 27, no. 2, pp. 293–305, 1991.

[17] R. S. Smith, C. C. Chu, and J. L. Fanson, "The design of $\mathcal{H}\infty$ controllers for an experimental noncollocated flexible structure problem," *IEEE Trans. Contr. Syst. Technol.*, vol. 2, pp. 101–109, Mar. 1994.

[18] L. Meirovitch, *Elements of Vibration Analysis*. New York: McGraw Hill, 1975.

[19] T. E. Alberts and J. A. Colvin, "Observations on the nature of transfer functions for control of piezoelectric laminates," *J. Intell. Mater. Syst. Structures*, vol. 8, no. 5, pp. 605–611, 1991.

[20] T. E. Alberts, T. V. DuBois, and H. R. Pota, "Experimental verification of transfer functions for a slewing piezoelectric laminate beam," *Control Eng. Practice*, vol. 3, no. 2, pp. 163–170, 1995.

[21] S. O. R. Moheimani and T. Ryall, "Considerations in placement of piezoceramic actuators that are used in structural vibration control," in *Proc. 38th IEEE Conf. Decision and Control*, Phoenix, AZ, Dec. 1999, pp. 1118–1123.

[22] S. O. R. Moheimani and M. Fu, "Spatial $\mathcal{H}_2$ norm of flexible structures and its application in model order selection," in *Proc. 37th IEEE Conf. Decision and Control*, Tampa, FL, Dec. 1998, pp. 3623–3624.

[23] K. Zhou, J. C. Doyle, and K. Glover, *Robust and Optimal Control*. Englewood Cliffs, NJ: Prentice-Hall, 1996.

[24] I. R. Petersen, B. D. O. Anderson, and E. A. Jonckheere, "A first principle solution to the nonsingular $\mathcal{H}_\infty$ control problem," *Int. J. Robust Nonlinear Control*, vol. 1, no. 3, pp. 171–185, 1991.

[25] S. Sana and V. S. Rao, "Robust control of input limited smart structural systems," *IEEE Trans. Contr. Syst. Technol.*, vol. 9, pp. 60–68, Jan. 2001.

[26] E. G. Eszter and C. V. Hollot, "An IQC for uncertainty satisfying both norm-bounded and passivity constraints," *Automatica*, vol. 33, no. 8, pp. 1545–11548, 1997.

[27] S. O. R. Moheimani, "Experimental verification of the corrected transfer function of a piezoelectric laminate beam," *IEEE Trans. Contr. Syst. Technol.*, vol. 8, pp. 660–666, July 2000.

Dunant Halim (S'99) was born in Jakarta, Indonesia, in 1974. He received the B.Eng. degree (first class honors) in aerospace engineering from the Royal Melbourne Institute of Technology, Melbourne, Australia, in 1999. He is currently pursuing the Ph.D. degree at the School of Electrical Engineering and Computer Science, University of Newcastle, Callaghan, Australia.

His research interests include smart structures, vibrations, and control theory.

S. O. Reza Moheimani (S'93–M'97–SM'00) was born in Shiraz, Iran in 1967. He received the B.Sc. degree from Shiraz University, in 1990 and the M.Eng.Sc. and Ph.D. degrees from the University of New South Wales, Sydney, Australia, in 1993 and 1996, respectively, all in electrical and electronics engineering.

In 1996, he was a Postdoctoral Research Fellow at the School of Electrical and Electronics Engineering, Australian Defense Force Academy, Canberra, Australia. In 1997, he joined the University of Newcastle, Callaghan, Australia, where he is currently a Senior Lecturer in the School of Electrical Engineering and Computer Science. He is an Associate Editor for *Control Engineering Practice*. He is currently serving on the editorial boards of several international conferences, including the 2nd International Federation of Automatic Control (IFAC) Conference on Mechatronic Systems, to be held in Berkeley, CA, in December 2002. His research interests include smart structures, mechatronics, control theory, and signal processing.

Dr. Moheimani is a Member of the Center for Integrated Dynamics and Control, an Australian Government Special Research Center, and the IFAC Technical Committee on Mechatronic Systems.